Influence of B, Al and Nb addition on the glass forming ability and stability of mechanically alloyed Zr-Ni amorphous alloys

WANG Yan[1*], DING JunFeng[1] & BAI YanWen[2]

[1] School of Materials Science and Engineering, University of Jinan, Jinan 250022, China;
[2] Key Laboratory for Liquid-Solid Structural Evolution and Processing of Materials of Ministry of Education, Shandong University, Jinan 250061, China

We investigated the influence of minor additions of B, Al and Nb that have representative atomic sizes on the glass forming ability (GFA) and stability of Zr-Ni amorphous alloys during mechanical alloying. The results show that the minor addition of B, Al or Nb does not shorten the initial time of the full amorphization reaction or improve the glass forming ability of the Zr-Ni alloys at a low rotation speed. However, B addition can effectively improve the mechanical stability of the amorphous phase against mechanically induced crystallization. Furthermore, the amorphous phase gradually transforms into a metastable fcc-phase with increasing milling time. The addition of Al and Nb that have similar atomic sizes has a similar effect on the GFA and the mechanical stability of the Zr-Ni amorphous phase. Moreover, Al and Nb addition can alter the crystallization behavior and improve the thermal stability of the Zr-Ni amorphous phase.

amorphous alloy, minor addition, mechanical alloying, glass forming ability, mechanical stability

Many researchers are interested in the origin of the glass forming ability (GFA) of amorphous alloys. Minor alloy additions or microalloying technologies have been important metallurgical practices and dominant concepts for the development of new metallic crystalline materials in the late half of the 20th century. It has recently been reported that appropriate minor additions are very effective in increasing GFAs and enhancing the thermal stability and mechanical properties of some metallic glasses [1–10]. Moreover, the minor addition approach also represents a feasible way to develop and design novel amorphous alloys. Our previous findings have shown that minor additions of single metalloid elements, metal elements or outphase amorphous alloys can effectively improve GFAs or enhance the mechanical stability of Zr-based alloys using mechanical alloying (MA) at given milling revolutions [11–15]. However, the mechanism of the minor addition has not been explained by fundamental theory in terms of glass formation and properties tailoring. It has been suggested that the additional atomic number, size mismatch or chemical affinity with constitutional elements may affect metallic glass formation and properties.

According to their atomic radii, elements that have been used for minor addition can be categorized into three groups [16]: large atoms (Zr, 0.16025 nm [17]), intermediate atoms (Al, 0.14317 nm, Nb, 0.14290 nm, and Ni, 0.12459 nm [17]) and small atoms (B, 0.082 nm [17]). In this paper, we aim to systematically investigate the effect of the small atom B, and the intermediate atoms Al and Nb with similar atomic sizes on the microstructural evolution of a mechanically alloyed $Zr_{66.7}Ni_{33.3}$ amorphous alloy under the same milling conditions. It should be noted that we selected a lower milling speed (150 r min^{-1}) compared to our previously reported experimental conditions (200 or 300 r min^{-1}). Therefore, the influence of minor additions and milling speed on the solid-state amorphization and phase evolution of Zr-Ni alloys is

*Corresponding author (email: mse_wangy@ujn.edu.cn)

discussed to further improve the GFA and the stability of Zr-Ni amorphous alloys.

1 Experimental

Powder mixtures of elemental Zr (<70 μm, 99.9 wt% purity), Ni(<70 μm, 99.5 wt% purity), B (<70 μm, 99.5 wt% purity), Al (<70 μm, 99.5 wt% purity) and Nb (<70 μm, 99.9 wt% purity) with nominal compositions of $Zr_{66.7-x}Ni_{33.3}M_x$ (M = B, Al, Nb and x = 0, 3 at%, 5 at%) were mechanically alloyed in a high energy ball mill (Fritsch P6) at a rotation speed of 150 r min⁻¹. A chromium steel vial and balls were used in this work. Mechanical alloying was carried out at room temperature in an Ar atmosphere with a ball-to- powder weight ratio of 15:1. To avoid an increase in the vial temperature, the milling procedure was periodically interrupted every 0.5 h and then halted for 0.5 h. In addition, the milling process was interrupted at various intervals to remove small amounts of the milled products for analysis and characterization. Structural characterization of the as-milled powders was carried out using a Rigaku

D/max-RB X-ray diffractometer (XRD) equipped with a Cu Kα radiation source, a Philips CM 20 transmission electron microscope (TEM) and a JEM-2100 high-resolution TEM (HRTEM). Thermal analysis of the as-milled samples was performed on a differential thermal analyzer (DTA) at a heating rate of 10 K min⁻¹.

2 Results

2.1 Effect of the small atom B

Figure 1 shows the XRD patterns of the as-milled $Zr_{66.7-x}Ni_{33.3}B_x$ (x = 0, 3at%, 5 at%) powders after selected MA times. The as-milled $Zr_{66.7}Ni_{33.3}$ sample at the initial stage (16 h) is just a polycrystalline mixture of starting reactant powders, and this is indicated by the sharp Bragg peaks that correspond to elemental Zr and Ni (Figure 1A(a)). With an increase in the milling time up to 32 h the as-milled powders are still composed of Zr and Ni but a broadening of the crystalline diffraction peaks is observed because of the decrease in grain size and an increase in the atomic level strain (Figure 1A(b)). After 48 h of MA all the Bragg peaks of the
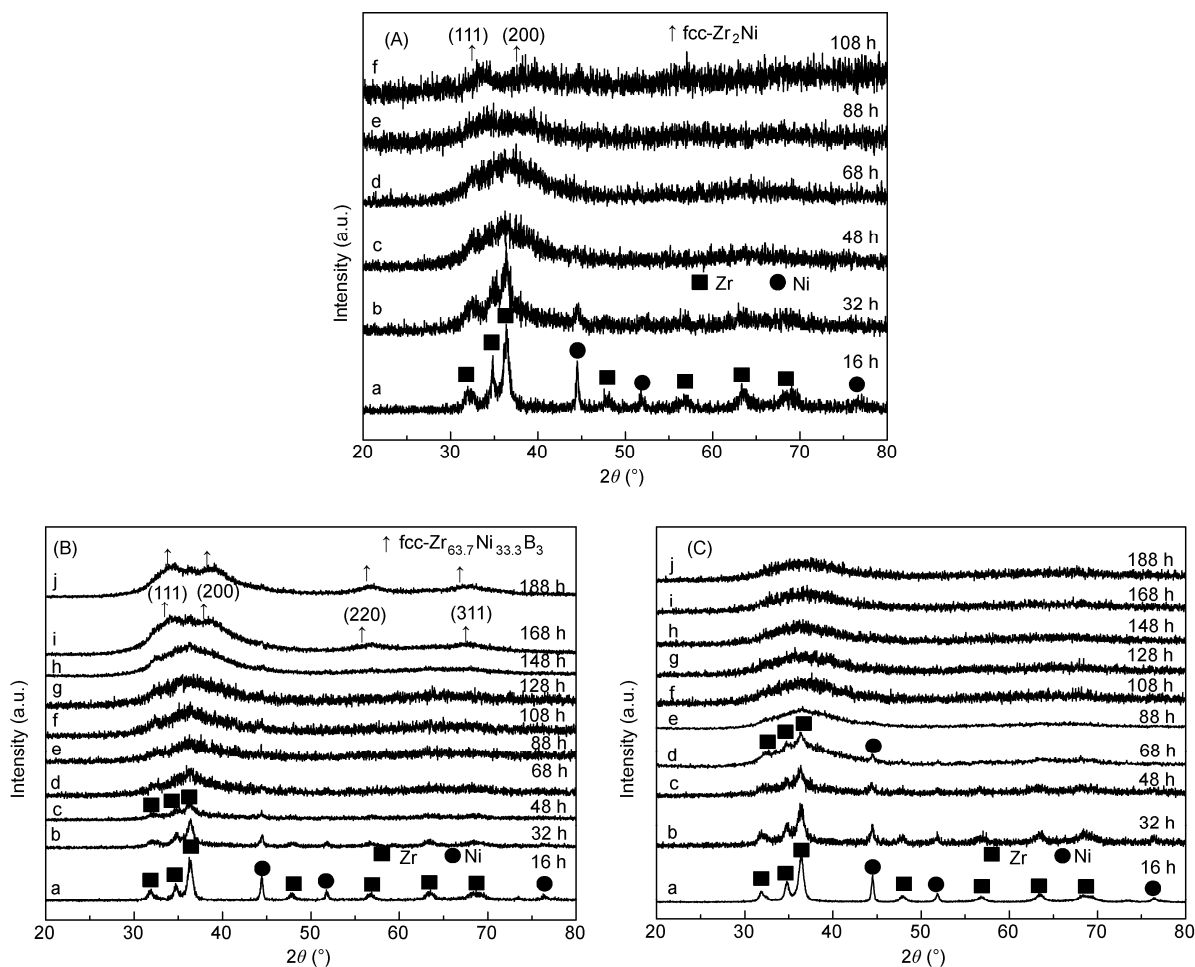

Figure 1 XRD patterns of the as-milled (A) $Zr_{66.7}Ni_{33.3}$, (B) $Zr_{63.7}Ni_{33.3}B_3$ and (C) $Zr_{61.7}Ni_{33.3}B_5$ powders after different MA times.

unprocessed elemental powders disappeared and a pronounced smooth halo appeared at $30° < 2\theta < 42°$ implying the formation of a single amorphous phase (Figure 1A(c)). To explore the stability of the formed $Zr_{66.7}Ni_{33.3}$ amorphous phase against MA the powders were continuously milled at up to 108 h under the same ball milling parameters, as shown in Figure 1A (d–f). With an increase in the milling time up to 108 h it is surprising that the amorphous phase begins to transform into a new metastable phase characterized by the diffraction peaks from the reflections of the (111) and (200) planes (Figure 1A(f)). An analysis of the Bragg peaks of the new phase confirms the formation of a metastable $fcc-Zr_2Ni$ phase ($fcc-Zr_2Cu$ structure [18]). The XRD patterns of the as-milled $Zr_{63.7}Ni_{33.3}B_3$ alloy are shown in Figure 1B. With an increase in the milling time to 48 h (Figure 1 B (c)) the milling products were found to still be composed of crystalline Zr and Ni. After 68 h of MA, a single amorphous phase was obtained in the as-milled product, as shown in Figure 1B (d). By increasing the MA time to 108 h the as-milled product was still a single amorphous phase (Figure 1B(e,f)). To explore the stability of the $Zr_{63.7}Ni_{33.3}B_3$ amorphous phase against MA the powders were continuously milled at up to 168 h under the same ball milling conditions (Figure 1 B (g–i)). Mechanical crystallization of the $Zr_{63.7}Ni_{33.3}B_3$ amorphous powders was found after 168 h of milling time. The amorphous phase partially transforms into a metastable $fcc-Zr_{63.7}Ni_{33.3}B_3$ phase, as indicated by the crystallization diffraction peaks for the (111),

(200), (220) and (311) planes, as shown in Figure 1B(i). An analysis of the Bragg peaks for the new phase confirms the formation of a metastable $fcc-Zr_{63.7}Ni_{33.3}B_3$ phase. By increasing the MA time to beyond 188 h the residual amorphous phase gradually devitrifies into the fcc phase and no other phase can be identified, as shown in Figure 1B(j). However, by increasing B addition up to 5 at%, a single amorphous phase appears at 88 h of milling time (Figure 1 C(e)). With an increase of the milling time up to 188 h the as-milled product is still a single amorphous phase, as shown in Figure 1C(f) to (j). This demonstrates that no mechanically induced crystallization occurs during the prolonged milling process, which is indicative of the high stability of the $Zr_{61.7}Ni_{33.3}B_5$ amorphous phase.

To verify the XRD results, some samples were selected to be examined using HRTEM. Figure 2 shows HRTEM images of the as-milled $Zr_{63.7}Ni_{33.3}B_3$ powders after 128 h and 188 h of MA time, respectively. Figure 2(a) shows an isotropic maze pattern for the $Zr_{63.7}Ni_{33.3}B_3$ powders after 128 h, which is typical of an amorphous structure. Figure 2(b) shows several nanocrystals with a size less than 10 nm embedded in the amorphous matrix of the $Zr_{63.7}Ni_{33.3}B_3$ powders after 188 h, as shown in the regions marked I, II and III. TEM observations further verify the above XRD results. Figure 3(a) shows a typical microstructure of the as-milled $Zr_{63.7}Ni_{33.3}B_3$ alloy after 188 h of MA. The selected-area electron diffraction (SAED) pattern consists of diffraction rings (Figure 3(b)), which is indicative of the
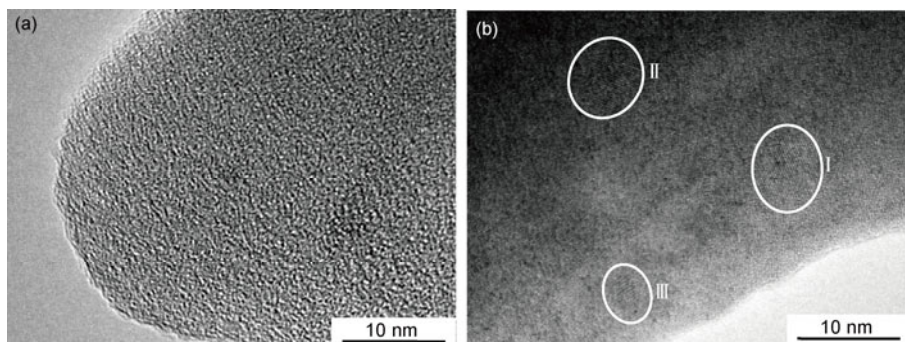

Figure 2 HRTEM images showing the microstructure of the as-milled $Zr_{63.7}Ni_{33.3}B_3$ powders after 128 h (a) and 188 h (b) of MA time.
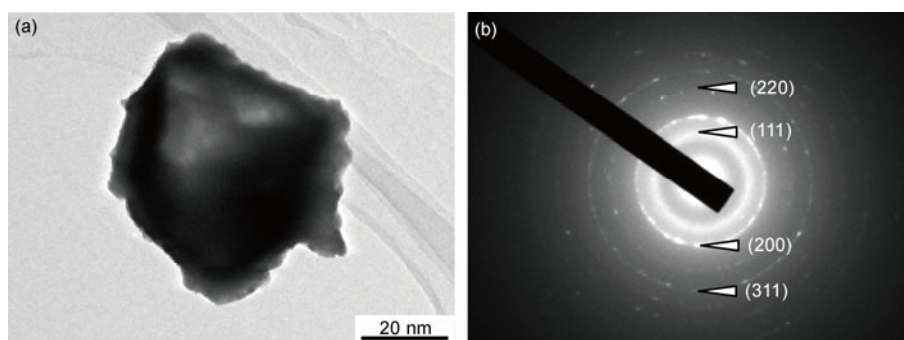

Figure 3 TEM image showing the microstructure of the as-milled $Zr_{63.7}Ni_{33.3}B_3$ powders (a) after 188 h of MA time. (b) SAED pattern corresponding to (a).

nanocrystalline characteristics of the corresponding microstructure. Furthermore, the SAED pattern also verifies that the nanocrystalline phase has an fcc-structure. In combination with the XRD result shown in Figure 1B(j), the nanocrystalline phase is fcc-$Zr_{63.7}Ni_{33.3}B_3$ and the diffraction rings from the (111), (200), (220) and (311) planes are also indexed in Figure 3(b).

Figure 4 shows DTA traces of the as-milled $Zr_{66.7-x}Ni_{33.3}B_x$ ($x = 0$, 3 at%, 5 at%) powders after 68 h of MA time. Each DTA trace shows three distinct exothermic peaks, corresponding to the crystallization of the amorphous phase. The crystallization peak temperature T_p, which is indicated by arrows does not vary significantly with B addition. Therefore, the addition of B cannot lead to an altered crystallization mode of the Zr-Ni amorphous alloys. Thus, we presume that B with a small atomic size is able to diffuse into the Zr-Ni matrix during MA. The solute B does not obviously cause a lattice distortion or alter the random configuration of Zr-Ni amorphous alloys. Therefore, B addition has no obvious effect on the crystallization mode of the Zr-Ni amorphous alloys.

2.2　Effect of the intermediate atoms Al and Nb with similar atomic sizes

Figure 5 shows the XRD patterns that were obtained from the $Zr_{63.7}Ni_{33.3}Al_3$, $Zr_{61.7}Ni_{33.3}Al_5$, $Zr_{63.7}Ni_{33.3}Nb_3$ and $Zr_{61.7}Ni_{33.3}Nb_5$ samples subjected to MA for different milling times. The structural evolution in those four alloys is similar to what was noted for the $Zr_{63.7}Ni_{33.3}B_3$ alloy that was milled for 88 h (Figure 5 A–D (a–e)). With an increase in the milling time of up to 108 h, however, two crystalline diffraction peaks appear at $2\theta = 30°$–$37°$ and $38°$–$42°$ on the XRD pattern of $Zr_{63.7}Ni_{33.3}Al_3$, and they overlap with a broad diffuse hump (Figure 5 A (f)). This indicates that the amorphous phase begins to show mechanical crystallization and transforms into a new metastable phase, which is characterized
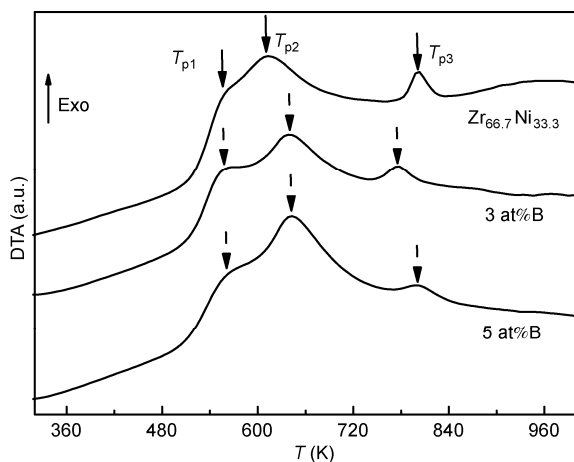

Figure 4　DTA traces of the as-milled $Zr_{66.7-x}Ni_{33.3}B_x$ ($x = 0$, 3 at%, 5 at%) powders after 68 h of MA time (The crystallization peak temperature T_p is indicated by arrows).

by the diffraction peaks from the reflections at (111) and (200). An analysis of the Bragg peaks of the new phase confirms the formation of a metastable fcc-$Zr_{63.7}Ni_{33.3}Al_3$ phase (fcc-Zr_2Cu structure [18]). However, by prolonging the MA time to 108 h the milling product of the $Zr_{61.7}Ni_{33.3}Al_5$, $Zr_{63.7}Ni_{33.3}Nb_3$ and $Zr_{61.7}Ni_{33.3}Nb_5$ samples was still full amorphous and it is stable and capable of withstanding the shear and impact stresses that are generated by the milling media (Figure 5 A–D(f)). The final milling time was 108 h for the Al and Nb addition, which is identical to that for $Zr_{66.7}Ni_{33.3}$ without addition. The initial mechanical crystallization time was 108 h for the 3 at% Al addition. Therefore, we did not prolong the milling time any further for the intermediate atom additions. It is necessary to further study the microstructural evolution of ZrNiAl and ZrNiNb during the milling process with an MA time longer than 108 h.

Figure 6 shows TEM image and SAED patterns of the as-milled $Zr_{63.7}Ni_{33.3}Al_3$ powders after 108 h of MA time. The particle in Figure 6(a) consists of several nanocrystals less than 50 nm in the amorphous matrix. The SAED pattern corresponding to area I shows a diffuse halo indicating the amorphous nature of this area (Figure 6(a-1)). The SAED pattern corresponding to area II verifies that the nanocrystalline phase has an fcc structure (Figure 6(a-2)). In combination with the XRD results shown in Figure 5 A(f) the nanocrystalline phase is the metastable fcc- $Zr_{63.7}Ni_{33.3}Al_3$ phase and the diffraction rings from the (111), (200) and (220) planes are also indexed in Figure 6(a-2).

To further investigate the effect of Al and Nb addition on the thermal stability of the Zr-Ni amorphous alloys, some samples were selected for examination by DTA. Figure 7 shows DTA traces of the as-milled $Zr_{66.7-x}Ni_{33.3}M_x$ (M = Al, Nb and $x = 0$, 3 at%, 5 at%) powders after 68 h of MA time. From Figure 7(b), (d) and (e), the Zr-Ni amorphous alloys with Al (3 at% and 5 at%) and Nb (5 at%) additions exhibit a distinct single-stage crystallization mode, which is different from the three-stage mode of $Zr_{66.7}Ni_{33.3}$ (Figure 7(a)) and the two-stage mode of $Zr_{63.7}Ni_{33.3}Nb_3$ (Figure 7(c)). T_{p1} shows a growing trend upon Al and Nb addition at the same milling time (68 h) as highlighted by the dashed arrows in Figure 7. To some extent, the addition of Al and Nb with intermediate atom sizes can alter the crystallization behavior and improve the thermal stability of the Zr-Ni amorphous alloys.

3　Discussion

Here, the termination time of the amorphization reaction (the formation time of a single amorphous alloy) during MA is defined as t_{fa}, which can be used to measure the GFA of the $Zr_{66.7-x}Ni_{33.3}M_x$ (M = B, Al, Nb and $x = 0$, 3 at%, 5 at%) alloys. According to our results (Figures 1 and 5) the t_{fa} values for the $Zr_{66.7-x}Ni_{33.3}M_x$ (M = B, Al, Nb and $x = 0$, 3 at%, 5 at%) alloys during MA were determined and are
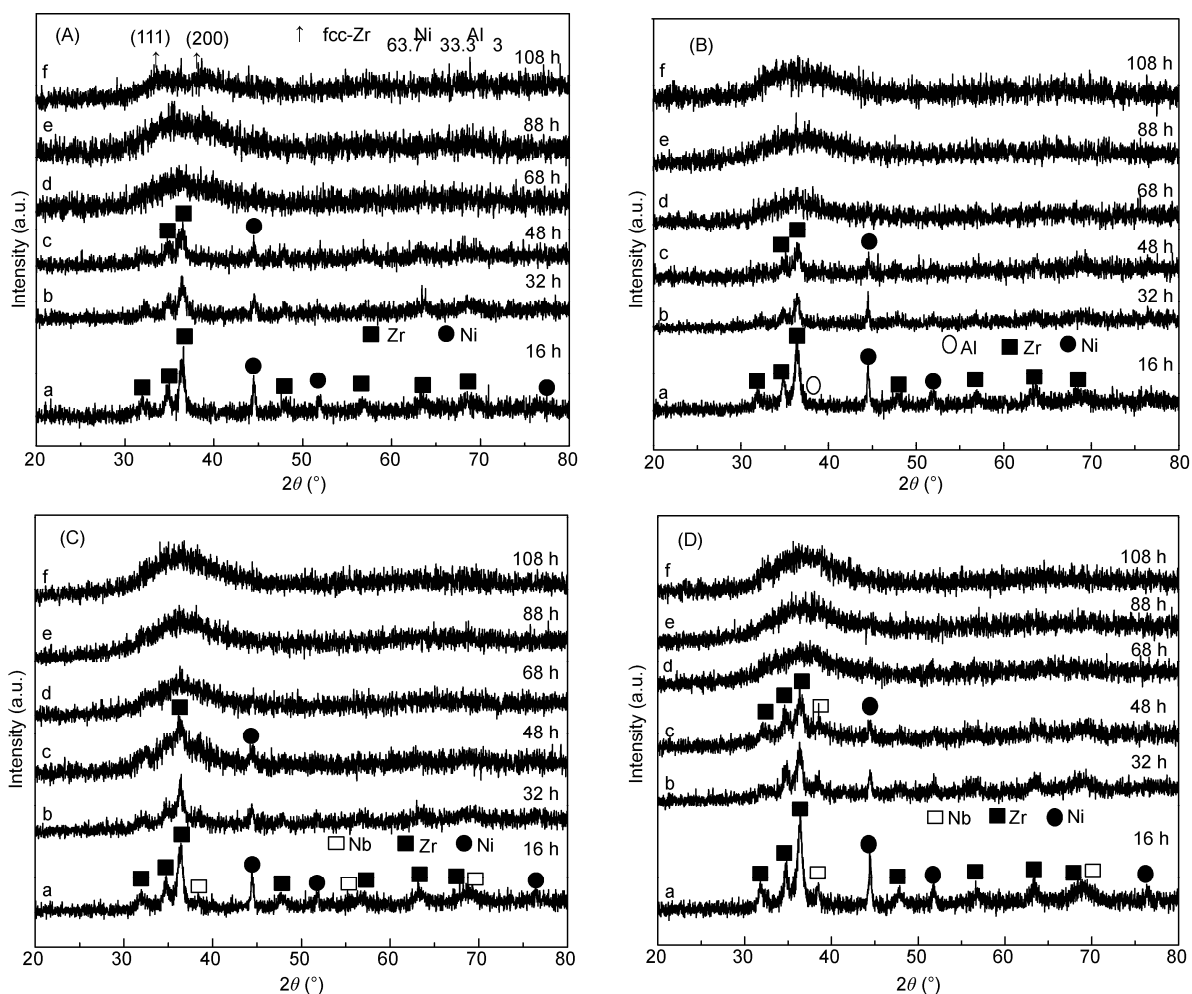
Figure 5 XRD patterns of the as-milled (A) $Zr_{63.7}Ni_{33.3}Al_3$, (B) $Zr_{61.7}Ni_{33.3}Al_5$, (C) $Zr_{63.7}Ni_{33.3}Nb_3$ and (D) $Zr_{61.7}Ni_{33.3}Nb_5$ powders after different MA times.
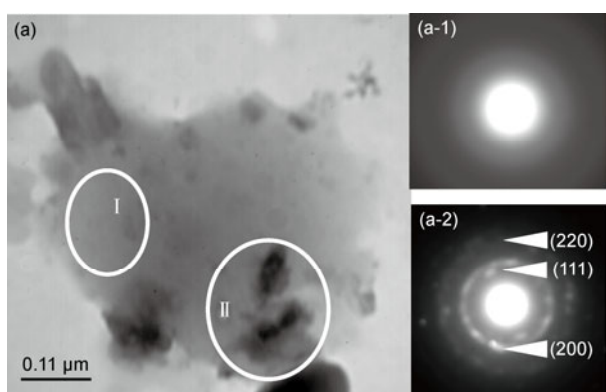

Figure 6 Typical bright field TEM image obtained from the as-milled $Zr_{63.7}Ni_{33.3}Al_3$ powders (a) after 108 h of MA time; (a-1) and (a-2) the corresponding SAED patterns obtained from the regions marked I and II in (a), respectively.

Figure 7 DTA traces of the as-milled $Zr_{66.7-x}Ni_{33.3}M_x$ (M = Al, Nb and x = 0, 3 at%, 5 at%) powders after 68 h of MA time (The crystallization peak temperature T_p is indicated by arrows).

listed in Table 1. B, Al and Nb addition does not shorten the t_{fa} and improve the GFA of the Zr-Ni alloys under ball milling conditions. For 5 at% B addition, the t_{fa} is 88 h, which is much longer than that of the $Zr_{66.7}Ni_{33.3}$ alloy. This demonstrates that small and intermediate atom additions are
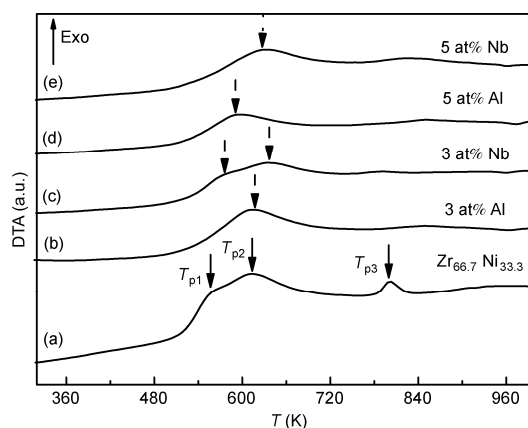
detrimental to the GFA of Zr-Ni alloys by MA at the lower milling speed (150 r min^{-1}). However, it is worth noting that a proper addition of small atom C [15] can significantly improve the GFA of Zr-Ni alloys at high milling speeds (200 or 300 r min^{-1}), as determined in our previous work.

Table 1 The termination time of the amorphization reaction (t_{fa}) and the lifespan of the amorphous phases (t_{sl}) for $Zr_{66.7-x}Ni_{33.3}M_x$ (M = B, Al, Nb and x = 0, 3, 5 at%) alloys under the same milling conditions

Alloys (at%)	t_{fa} (h)	t_{sl} (h)
$Zr_{66.7}Ni_{33.3}$	48	60
$Zr_{63.7}Ni_{33.3}B_3$	68	100
$Zr_{61.7}Ni_{33.3}B_5$	88	>100
$Zr_{63.7}Ni_{33.3}Al_3$	68	40
$Zr_{61.7}Ni_{33.3}Al_5$	68	>40
$Zr_{63.7}Ni_{33.3}Nb_3$	68	>40
$Zr_{61.7}Ni_{33.3}Nb_5$	68	>40

The rotation speed of ball milling has a significant influence on the formation of the amorphous phase by MA [13]. The velocity and impact frequency of the milling balls increase with an increase in the rotation speed. During milling, the relationship between the average velocity v_b, the average impact frequency f and the rotation speed Ω can be expressed as [19]:

$$v_b = \frac{a_1 + 4a_2\left[a_3 + m_p\left(1 + R_{Bp}\right)\right]}{a_4\left[a_3 + m_p\left(1 + R_{Bp}\right)\right]} a_5\Omega, \tag{1}$$

$$f = \frac{a_1 + 4a_2\left[a_3 + m_p\left(1 + R_{Bp}\right)\right]}{b_1\left[a_3 + m_p\left(1 + R_{Bp}\right)\right]r_b}(m_p R_{BP})^{1/3} a_5\Omega, \tag{2}$$

where a_1–a_5 and b_1 are constants related to the geometric size and quality of the ball mill and the vial, m_p is the powder weight, R_{BP} is the ball-to-powder weight ratio and r_b is the radius of the milling balls. Eqs.(1) and (2) indicate that v_b and f are proportional to the rotation speed. Firstly, increasing the rotation speed can improve the velocity of the milling balls and thus enhance the energy of the powders that are transferred by the impact behavior of the balls. Secondly, an increase in rotation speed can improve the collision frequency of the milling balls and also increase the energy captured by the powders, which can enhance the diffusion driving force among the atoms and accelerate the solid-state reaction. Therefore, the rotation speed plays an important role in the formation of an amorphous phase by MA. Small atom B cannot easily occupy interstitial free space among the major constituent atoms because of the weaker shear and impact forces generated by the milling media using the lower milling speed (150 r min⁻¹). Thus, B addition does not result in a more confusional atomic arrangement and it decreases the GFA of the Zr-Ni alloy under these experimental conditions. Intermediate atoms of Al and Nb, which have a marginal mismatch of atomic sizes between Zr and Ni are unable to introduce strain into the crystal lattice and are ineffective in enhancing the GFA. However, the effect of Al and Nb on improving the atomic packing density is better than that of small atom B. The addition of Al and Nb does not obviously decrease the GFA

with an increase in content to 5 at% and their t_{fa} values are still 68 h.

Here, the lifespan (stability) of the Zr-Ni amorphous phases (t_{sl}) was used to study the effect of B, Al and Nb addition on the microstructural evolution of the Zr-Ni amorphous phase. Table 1 lists the lifespan of the amorphous phases obtained under the same milling conditions. The t_{sl} value of the $Zr_{66.7}Ni_{33.3}$ amorphous phase is 60 h. The t_{sl} value increases to more than 100 h with an increase in B addition. B addition can greatly enhance the mechanical stability of the Zr-Ni amorphous phases. Because of its strong atomic bonding with metallic elements, small additions of metalloid atoms can enhance the short-range compositional order. Therefore, the mechanical stability of the amorphous phase improves. Therefore, the rearrangement of atoms in the $Zr_{66.7-x}Ni_{33.3}B_x$ (x = 3 at%, 5 at%) alloys becomes much more difficult. However, Al addition (3 at%) shortens the lifespan (40 h) and decreases the mechanical stability of the Zr-Ni amorphous phases. This can be explained by considering the diffusivity of intermediate atoms in Zr-Ni. Al atoms have a faster diffusivity in Zr-Ni and will promote the mechanically induced crystallization of the amorphous phase to some extent. The effect of Al (5 at%) and Nb (3 at%, 5 at%) addition on mechanical stability is better than that of 3 at% Al addition.

4   Conclusions

The minor addition of B, Al and Nb does not decrease the initial time of the full amorphization reaction and has a negligible influence on the GFA of Zr-Ni alloys during MA at a low rotation speed. However, small atom B addition can obviously increase the mechanical stability of the Zr-Ni-B amorphous phase against mechanically induced crystallization during ball milling. Moreover, B addition has no obvious effect on the crystallization mode of the Zr-Ni amorphous alloys. The addition of Al and Nb with similar atomic sizes shows a similar effect on the GFA and the mechanical stability of the Zr-Ni amorphous phase. Moreover, Al and Nb addition can alter the crystallization behavior and improve the thermal stability of the Zr-Ni amorphous alloys.

1   Wang W H. Roles of minor additions in formation and properties of bulk metallic glasses. Prog Mater Sci, 2007, 52: 540–596

2   Xi X K, Li L L, Wang W H, et al. Correlation of atomic cluster symmetry and glass-forming ability of metallic glass. Phys Rev Lett, 2007, 99: 095501

3   Zhang B, Wang R J, Wang W H, et al. Formation of cerium-based bulk metallic glasses. Acta Mater, 2006, 54: 3025–3032

4   Liu C T, Lu Z P. Effect of minor alloying additions on glass formation in bulk metallic glasses. Intermatallics, 2005, 13: 415–418

5   Qiang J B, Zhang W, Inoue A. Effects of Al and Ti additions on the thermal stability, glass-forming ability and mechanical properties of $Ni_{60}Nb_{20}Zr_{20}$ glassy alloy. Mater Sci Eng B, 2008, 148: 114–118

6   Mishra D, Perumal A, Saravanan P, et al. Effect of Co or Mn addition on the soft magnetic properties of amorphous $Fe_{89-x}Zr_{11}B_x$ (x=5, 10) alloy ribbons. J Magn Magn Mater, 2009, 321: 4097–4102

7   Sha P F, Qi Z, Zhang Z H. Effect of Ag or Pd additions on the microstructure, crystallization and thermal stability of Al-Ni-Ce amorphous alloys. Intermetallics, 2010, 18: 1699–1706

8   Marcin G N, Marcin J D, Michał S, et al. Investigation of the thermal and magnetic properties of $Fe_{61}Co_{10}Zr_2Fe_{61}Co_{10}Zr_{2.5}Hf_{2.5}Me_2 W_2B_{20}$ (Me = Y, Nb, W, Ti, Mo, Ni) bulk amorphous alloys obtained by an induction suction method. J Alloys Compd, 2011, 509: 3382–3386

9   Jiao Z B, Li H X, Wu Y, et al. Effects of Mo additions on the glass-forming ability and magnetic properties of bulk amorphous Fe-C-Si-B-P-Mo alloys. Sci China Phys Mech Astron, 2010, 53: 430–434

10   Zhong Y, Zhou Y J, Hui X D, et al. Minor alloying behavior in bulk metallic glasses and high-entropy alloys. Sci China Ser G-Phys Mech Astron, 2008, 51: 427–434

11   Wang Y, Geng H R, Wang Y Z. Influence of outphase $Cu_{50}Ti_{50}$ amorphous alloy addition on microstructural evolution of mechanically alloyed $Zr_{66.7}Ni_{33.3}$ amorphous alloy. J Non-Cryst Solids, 2011, 357: 78–82

12   Wang Y, Wang J F, Li C C. Effect of La addition on glass-forming ability and stability of mechanically alloyed Zr-Ni amorphous alloys. Mater Sci Eng A, 2011, 528: 1623–1627

13   Wang Y, Chen X X, Geng H R, et al. Amorphization and crystallization of $Zr_{66.7-x}Cu_{33.3}Nb_x$ (x=0, 2, 4) alloys during mechanical alloying. J Alloy Compd, 2009, 474: 152–157

14   Wang Y, Geng H R, Wang Y Z. Influence of minor addition of Pd, Ag or Au on the microstructural evolution of mechanically alloyed Zr-Ni alloys. J Non-Cryst Solid, 2009, 355: 464–467

15   Wang Y, Geng H R, Yang Z X, et al. Effect of carbon on the microstructural evolution of $Zr_{66.7-x}Ni_{33.3}C_x$ (x = 0, 1, 3) alloys during mechanical alloying. J Non-Cryst Solid, 2008, 354: 3984–3989

16   Lu Z P, Liu C T. Role of minor alloying additions in formation of bulk metallic glasses: A Review. J Mater Sci, 2004, 39: 3965–3974

17   Senkov O N, Miracle D B. Effect of the atomic size distribution on glass forming ability of amorphous metallic alloys. Mater Res Bull, 2001, 36: 2183–2198

18   El-Eskandarany M S, Inoue A. Solid-state crystalline-glassy cyclic phase transformations of mechanically alloyed $Cu_{33}Zr_{67}$ powders. Metall Trans A, 2002, 33: 135–143

19   Yang J Y, Zhang T J, Cui K, et al. Analysis of impact behavior during ball milling. Acta Metall Sin, 1997, 33: 381–385